AIAA JOURNAL
Vol. 39, No. 1, January 2001

Unified Approach to Modeling Matrix Cracking and Delamination in Laminated Composite Structures

Robert Thornburgh* and Aditi Chattopadhyay†
Arizona State University, Tempe, Arizona 85287-6106

A higher-order theory is developed to model the behavior of composite laminates with delamination and transverse matrix cracking. The higher-order displacement field is used in the sublaminates for accurate representation of the effects of transverse shear. This also allows description of the independent displacement fields above and below the delamination. A refined displacement field is obtained through the satisfaction of stress-free boundary conditions at all free surfaces, including delaminated interfaces. The effect of matrix cracking is determined using a separate finite element model of a representative crack and implemented into the structural model by means of reduced laminate stiffnesses. Matrix crack closure creates a bimodularity where stiffness under compression is greater than stiffness under tension. This bimodularity is addressed using an iterative process. The effect of this bimodularity on mode shapes is shown to be small, and a method is presented for determining natural frequencies in the presence of matrix cracks. Results show that this model provides a consistent level of accuracy for a variety of laminate materials and configurations, with various combinations of delaminations and matrix cracks.

Nomenclature

A, B, D, E, F, H	=	plate stiffness matrices
$\bar{A}, \bar{B}, \bar{D}, \bar{E}, \bar{F}, \bar{H}$	=	effective plate stiffness matrices with matrix cracks
C, C_0	=	in-plane and out-of-plane higher-order stiffness matrices
e, e_0	=	in-plane and out-of-plane engineering strain
h	=	laminate thickness
l_k	=	total crack length in kth layer
N, M, P	=	in-plane stress resultants
Q, R	=	out-of plane stress resultants
T	=	global–local laminate transformation matrix
t_k	=	thickness of kth ply
u_0, v_0, w_0	=	midplane displacements
u_1, u_2, u_3	=	displacements along x, y, and z directions
W	=	total work
z	=	location relative to laminate midplane
z_k	=	distance of kth layer midplane from laminate midplane
$\alpha^d, \gamma^d, \delta^l$	=	geometric parameters for continuity conditions
β, β_0	=	higher-order crack behavior matrices
$\varepsilon^0, \kappa^0, \kappa^2$	=	coefficients of the strain equations
ρ_k	=	crack density in kth layer
σ, σ_0	=	in-plane and out-of-plane stress
τ, τ_0	=	crack face stresses
ψ_x, ψ_y	=	rotations of the normals to midplane about y and x axes
Ω	=	total in-plane area
ω	=	natural frequency
ω_1, ω_2	=	natural frequency for first and second half-cycles

I. Introduction

MATRIX cracking is a common form of damage in composite laminates and results from a variety of conditions including low-velocity impact, fatigue, and excessive loading. Matrix cracks can open under load, thus creating an increase in the perceived strains of a laminate and a reduction in the effective stiffness. In engineering design it is often assumed that once matrix cracking has initiated, the lamina with cracks is no longer capable of carrying load. This technique is known as the ply discount method. However, the cracked layer is in reality still carrying some of the load, and thus the reduction in laminate stiffness will be a function of crack density. Being able to describe the changes in structural behavior accurately will allow designers to predict the effects of localized damage on static and dynamic characteristics. Also, the modeling of matrix cracking is necessary for the development of smart composite structures capable of detecting damage.

A large amount of research has been conducted to model the effects of transverse matrix cracking on the stiffness of composite laminates. Some models are closed-form solutions,[1,2] whereas others rely on experimental data to determine key parameters in the solution.[3] Also, most models are applicable to pure extension, and only a few address the changes in matrix crack behavior under bending loads.[4–6] The behavior under shear loading has received some attention,[1,2,5,7] which is vital to describing the changes in angle ply structures. However, transverse shear has received much less attention.[8] Finally, less work has been reported on applying the available models to actual structures and addressing the complications created by crack closure.

Delamination is known to reduce significantly the natural frequencies of laminated plates and has been studied by a number of authors.[9–16] Delamination generally is formed by the same conditions that result in matrix cracks, and matrix cracking is usually the precursor to delamination created by fatigue. However, the effects of delamination are usually considered independently, without considering matrix cracking. Modeling of delamination has been done using a variety of approaches. Three-dimensional models[9] provide accurate results, whereas two-dimensional models[10,11] are more computationally efficient. Layerwise theories[12] have also been used, but the computational effort can be quite large for thick laminates with a large number of layers. A refined higher-order theory was developed by Chattopadhyay and Gu,[13] and it has been shown to be efficient and provide accurate solutions.[14–15] Therefore the current research builds on this model.

Thus, the objective of this research is to develop a model that is capable of describing the effect of delamination and matrix cracking in a composite plate, of arbitrary laminate configuration, with consistent accuracy for a wide variety of laminate materials. The developed theory is capable of describing the effect of all three modes of crack behavior and is applicable to extensional, bending,

Received 27 October 1999; revision received 15 April 2000; accepted for publication 30 May 2000.

*Graduate Research Associate, Department of Mechanical and Aerospace Engineering. Student Member AIAA.
†Professor, Department of Mechanical and Aerospace Engineering. Associate Fellow AIAA.

and transverse loading conditions. This model is used to investigate both static and dynamic response of composite laminates.

II. Matrix Cracking

The study of matrix cracking is based on the assumption that cracks can be modeled as a statistically uniform array spaced at some average distance. Unlike other studies that attempt to predict the amount of damage based on loading history, in this study, it is assumed that the damage is known. The cracking can be in any combination of layers including the surface layers of the laminate. The effects of matrix cracking must be developed to reflect the structural model used. If only the effects of mode 1 and 2 crack opening are considered, then the results would then only be appropriate for classical plate models where transverse shear is not considered. For moderately thick plates modeled using a first-order shear deformation theory, the transverse shear plays a role in plate deflection, and, therefore, mode 2 crack behavior must be determined. Higher-order plate theories[13] more accurately represent the distribution of transverse shear, but because they have additional higher-order parameters, the effect of matrix cracking on these parameters must also be determined. The higher-order displacement field, however, has the advantage that it provides for a quadratic distribution of transverse shear through the thickness, but does not require any more parameters than the first-order shear deformation theory, which assumes a constant distribution of transverse shear.

Consider a composite plate of arbitrary thickness in the presence of matrix cracking (Fig. 1). To model the displacement field, a refined higher-order theory is used. The procedure is capable of accurately predicting the transverse shear stresses through the thickness while being computationally efficient. The displacement field for a plate of thickness h is as follows:

$$u_1 = u_0 + z\psi_x - \frac{4z^3}{3h^2}\left(\psi_x + \frac{\partial w}{\partial x}\right) \tag{1a}$$

$$u_2 = v_0 + z\psi_y - \frac{4z^3}{3h^2}\left(\psi_y + \frac{\partial w}{\partial y}\right) \tag{1b}$$

$$u_3 = w_0 \tag{1c}$$

The quantities u, v, and w are the displacements of a point on the midplane. The displacement field satisfies the traction-free boundary condition, where τ_{xz} and τ_{yz} are zero on the upper and lower surfaces of the plate. The strains then assume the following form:

$$e_m = \varepsilon_m^0 + z\left(\kappa_m^0 + z^2\kappa_m^2\right), \qquad m = 1, 2, 6 \tag{2a}$$

$$e_n = \varepsilon_n^0 + z^2\kappa_n^2, \qquad n = 4, 5 \tag{2b}$$

$$e_3 = 0 \tag{2c}$$

where ε^0, κ^0, and κ^2 are coefficients expressed as functions of u, v, w, ψ_x, and ψ_y. For convenience the stress and strains are separated into in-plane and out-of-plane components:

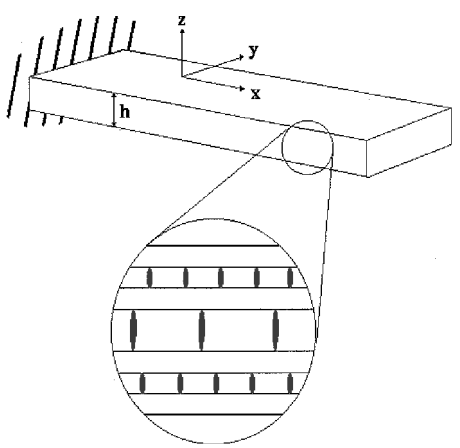

Fig. 1 Cracked composite plate.

$$\sigma = \begin{Bmatrix}\sigma_1\\ \sigma_2\\ \sigma_6\end{Bmatrix}, \qquad e = \begin{Bmatrix}e_1\\ e_2\\ e_6\end{Bmatrix}, \qquad \varepsilon^0 = \begin{Bmatrix}\varepsilon_1^0\\ \varepsilon_2^0\\ \varepsilon_6^0\end{Bmatrix}$$

$$\kappa^0 = \begin{Bmatrix}\kappa_1^0\\ \kappa_2^0\\ \kappa_6^0\end{Bmatrix}, \qquad \kappa^2 = \begin{Bmatrix}\kappa_1^2\\ \kappa_2^2\\ \kappa_6^2\end{Bmatrix} \tag{3a}$$

$$\sigma_0 = \begin{Bmatrix}\sigma_4\\ \sigma_5\end{Bmatrix}, \qquad e_0 = \begin{Bmatrix}e_4\\ e_5\end{Bmatrix}, \qquad \varepsilon_0^0 = \begin{Bmatrix}\varepsilon_4^0\\ \varepsilon_5^0\end{Bmatrix}$$

$$\kappa_0^0 = \begin{Bmatrix}\kappa_4^0\\ \kappa_5^0\end{Bmatrix}, \qquad \kappa_0^2 = \begin{Bmatrix}\kappa_4^2\\ \kappa_5^2\end{Bmatrix} \tag{3b}$$

This notation allows convenient expression of the stress strain relations in matrix form and separation of the in-plane and out-of-plane effects. The constitutive equations for the undamaged and the cracked laminate are

$$\begin{Bmatrix}N\\ M\\ P\end{Bmatrix} = \begin{bmatrix}A & B & E\\ B & D & F\\ E & F & H\end{bmatrix}\begin{Bmatrix}\varepsilon^0\\ \kappa^0\\ \kappa^2\end{Bmatrix} = \begin{bmatrix}\bar{A} & \bar{B} & \bar{E}\\ \bar{B} & \bar{D} & \bar{F}\\ \bar{E} & \bar{F} & \bar{H}\end{bmatrix}\begin{Bmatrix}\varepsilon^0\\ \kappa^0\\ \kappa^2\end{Bmatrix} \tag{4a}$$

$$\begin{Bmatrix}Q\\ R\end{Bmatrix} = \begin{pmatrix}A & D\\ D & F\end{pmatrix}\begin{Bmatrix}\varepsilon_0^0\\ \kappa_0^0\end{Bmatrix} = \begin{pmatrix}\bar{A} & \bar{D}\\ \bar{D} & \bar{F}\end{pmatrix}\begin{Bmatrix}\varepsilon_0^0\\ \kappa_0^0\end{Bmatrix} \tag{4b}$$

where A, B, D, E, F, and H are the plate stiffnesses derived as follows:

$$(A, B, D, E, F, H) = \int_{-h/2}^{h/2} \bar{Q}(1, z, z^2, z^3, z^4, z^6)\,dz \tag{5}$$

where $\bar{Q}$ is the global stiffness matrix for each ply. The A, B, and D matrices are the same as those used in classical plate theory, and the E, F, and H matrices have the same relationship extended to the higher-order functions of z. N, M, P, Q, and R are the stress resultants defined by

$$(N, M, P) = \int_{-h/2}^{h/2} \sigma(1, z, z^3)\,dz \tag{6a}$$

$$(Q, R) = \int_{-h/2}^{h/2} \sigma_0(1, z^2)\,dz \tag{6b}$$

In Eqs. (4a) and (4b), the quantities with the overbar refer to the effective strains and stiffness values for the cracked laminate. These reduced stiffness values must be determined to analyze the complete system. For simplification purposes, Eq.(4) is represented as follows:

$$\begin{Bmatrix}N\\ M\\ P\end{Bmatrix} = Ce = \bar{C}\bar{e}, \qquad \begin{Bmatrix}Q\\ R\end{Bmatrix} = C_0 e_0 = C_0 e_0 \tag{7}$$

where C and C_0 are the 9×9 and 4×4 higher-order stiffness matrices, and e and e_0 are the in-plane and out-of-plane strain components.

To determine the effects of matrix cracking, a procedure similar to that developed by Adolfsson and Gudmundson[5] is used. However, unlike their work, which relies on fracture mechanics and the assumption of the crack being in an infinite homogeneous medium, the current technique uses a finite element approach based on the actual laminate configuration. Also, the model developed by Adolfsson and Gudmundson[5] is based on the classical plate theory, which ignores transverse shear stresses. Because a higher-order model is used in this paper, additional parameters need to be determined.

With the principle of superposition, the effective strains in the cracked laminate are equal to the summation of strains in an uncracked laminate and the strains resulting from the application of

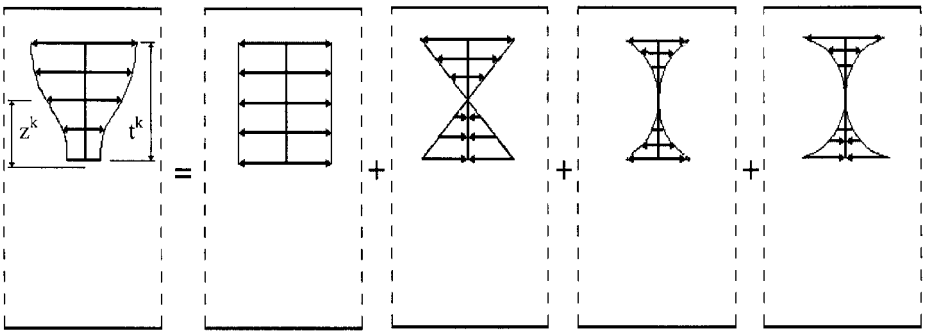

Fig. 2 Higher-order stress distribution on the crack face.

stresses on the crack face (Fig. 2). The stresses correspond to σ_2, σ_4, and σ_6 in the local coordinate system, and to mode 1–3 crack loading. For the kth layer, this loading can easily be separated into components as follows.

For modes 1 and 3:

$$\tau = \tau_0 + \tau_1\eta + \tau_2\eta^2 + \tau_3\eta^3 \tag{8}$$

For mode 2:

$$\tau_0 = \tau_{00} + \tau_{01}\eta + \tau_{02}\eta^2 \tag{9}$$

$$\eta = (z - z_k)/(t_k/2) \tag{10}$$

where t_k is the thickness of the cracked layer. Thus, the stresses on the crack face, τ and τ_0, are cubic and quadratic functions, respectively. These components are defined based on the strains in Eqs. (2a–2c) as follows:

$$\tau_0 = TQ\left(\varepsilon^0 + z_k\kappa^0 + z_k^3\kappa^2\right) \tag{11a}$$

$$\tau_1 = (t_k/2)TQ\left(\kappa^0 + 3z_k^2\kappa^2\right) \tag{11b}$$

$$\tau_2 = \left(3t_k^2 \mid 4\right)TQz_k\kappa^2 \tag{11c}$$

$$\tau_3 = \left(t_k^3 \mid 8\right)TQ\kappa^2 \tag{11d}$$

$$\tau_{00} = TQ\left(\varepsilon_0^0 + z_k^2\kappa_0^2\right) \tag{12a}$$

$$\tau_{01} = t_kTQz_k\kappa_0^2 \tag{12b}$$

$$\tau_{02} = \left(t_k^2 \mid 4\right)TQ\kappa_0^2 \tag{12c}$$

By the defining of matrices β and βo

$$\beta = \begin{bmatrix} \beta_{00} & \beta_{01} & \beta_{02} & \beta_{03} \\ \beta_{10} & \beta_{11} & \beta_{12} & \beta_{13} \\ \beta_{20} & \beta_{21} & \beta_{22} & \beta_{23} \\ \beta_{30} & \beta_{31} & \beta_{32} & \beta_{33} \end{bmatrix}, \qquad \beta o = \begin{bmatrix} \beta o_{00} & \beta o_{01} & \beta o_{02} \\ \beta o_{10} & \beta o_{11} & \beta o_{12} \\ \beta o_{20} & \beta o_{21} & \beta o_{22} \end{bmatrix} \tag{13}$$

and assuming that the work done in one cracked layer is not affected by cracking in other layers, the change in work for the kth cracked layer can be expressed as

$$\Delta W_k = \left(t_k^2 l_k \mid 2\right)\tau_k^T\beta_k\tau_k \tag{14}$$

where l_k is the total crack length in that layer, which can be written in the more familiar form as

$$l_k = \Omega\rho_k/t_k \tag{15}$$

In Eq. (15), Ω is the total plate in-plane area. The crack density ρ_k is defined as the ratio of layer thickness to crack spacing.[17] The total work W for the cracked plate can now be described as follows:

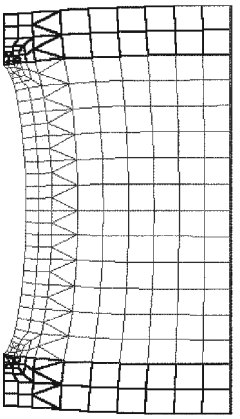

Fig. 3 Finite element mesh for representative crack.

$$W = \frac{\Omega}{2}\left[\bar{e}^T C\bar{e} - \sum_{k=1}^{N} t_k\rho_k\tau_k^T\beta_k\tau_k\right] + \frac{\Omega}{2}\left[e_0{}^T C_0 e_0 - \sum_{k=1}^{N} t_k\rho_k\tau_{0k}^T\beta o_k\tau_{0k}\right] = \frac{\Omega}{2}\left(\bar{e}^T\bar{C}\bar{e} + e_0{}^T C_0 e_0\right) \tag{16}$$

The quantities that need to be determined are the elements in matrices β and βo. Adolfsson and Gudmundson[5] used fracture mechanics solutions based on stress intensity factors to relate the load to the work done. Because of the difficulty in obtaining fracture mechanics solutions, it was necessary to use the solutions for cracks in infinite homogeneous media. The accuracy of this assumption varies dramatically based on laminate thickness and material properties. To develop a more reliable approach, a separate finite element analysis is used to relate the individual loads to changes in work. This was done by applying each load τ_n to a finite element mesh representing the composite cross section around a single crack with appropriate boundary conditions. The work due to extensional, bending, and shear deformation is determined based on mesh displacements (Fig. 3). The values of the elements in matrices β and βo are then derived by using Eq. (14).

The separate finite element modeling of the crack behavior in each layer with cracks causes definite increases in the computational effort. However, the developed procedure offers advantages that can offset this increase in CPU time. First, the β matrix can be derived for a number of different crack densities, then a simple curve-fitting process can be used to express β as a function of crack density. Second, this function can then be stored and reused if the same laminate configuration is encountered again. Therefore, although a significant amount of computational effort is required the first time a new material or laminate configuration is used, subsequent analyses will require very minimal calculations.

III. Delamination Modeling

To incorporate delamination, the structure is divided into regions, as seen in Fig. 4. Equations (1a–1c) are applied to each region

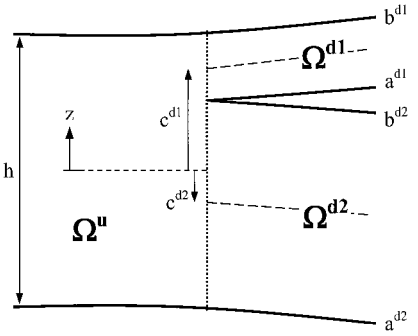

Fig. 4 Delaminated composite cross section.

(Ω^r $r = u, d1, d2$). The displacement field now assumes the following form:

$$u_1^r = u_0^r + (z - c^r)\left(\phi_x^r - \frac{\partial w^r}{\partial x}\right) - \frac{4(z - c^r)^3}{3h^2}\phi_x^r \quad (17a)$$

$$u_2^r = v_0^r + (z - c^r)\left(\phi_y^r - \frac{\partial w^r}{\partial y}\right) - \frac{4(z - c^r)^3}{3h^2}\phi_y^r \quad (17b)$$

$$u_3^r = w_0^r \quad (17c)$$

where c^r is the local midplane of each region. Continuity conditions are imposed on the interfaces between the undelaminated region and the sublaminates.

$$u^u = u^{d1}, \qquad a^{d1} \le z \le b^{d1} \quad (18a)$$

$$u^u = u^{d2}, \qquad a^{d2} \le z \le b^{d2} \quad (18b)$$

Because the displacement distribution is nonlinear, Eqs. (18a) and (18b) cannot be satisfied exactly and must instead be satisfied in an average sense. An error function for the first sublaminate is defined as

$$e_{\text{error}} = u^u - u^{d1}, \qquad a^{d1} \le z \le b^{d1} \quad (19)$$

The difference between u^u and u^{d1} is then minimized by integrating the square of the error over the thickness. The derivatives with respect to the independent functions in region Ω^{d1} (Fig. 4) are then set to zero. This yields the following relationships:

$$u_0^{d1} = u_0^u + (c^u - c^{d1})\frac{\partial w^u}{\partial x} + \alpha^{d1}\phi_x^u \quad (20a)$$

$$v_0^{d1} = v_0^u + (c^u - c^{d1})\frac{\partial w^u}{\partial y} + \alpha^{d1}\phi_y^u \quad (20b)$$

$$w_0^{d1} = w_0^u \quad (20c)$$

$$\frac{\partial w^{d1}}{\partial x} = \frac{\partial w^u}{\partial x} + \gamma^{d1}\phi_x^u \quad (20d)$$

$$\frac{\partial w^{d1}}{\partial y} = \frac{\partial w^u}{\partial y} + \gamma^{d1}\phi_y^u \quad (20e)$$

$$\phi_x^{d1} = \delta^{d1}\phi_x^u \quad (20f)$$

$$\phi_y^{d1} = \delta^{d1}\phi_y^u \quad (20g)$$

The constants α^{d1}, γ^{d1}, and δ^{d1} are defined in the Appendix. Identical expressions corresponding to region Ω^{d2} (Fig. 4) are similarly formulated.

IV. Composite Plate Modeling

Modeling of a composite plate with matrix cracking and delamination will be accomplished using the following steps. Reduced stiffness values will be determined for layers containing matrix cracks using the separate finite element model described earlier. Each cracked layer will be analyzed individually and given its own reduced stiffness values. The plate will then be modeled using the higher-order theory and the finite element method. Once the finite element stiffness matrix for the plate is formed, continuity conditions will be enforced between the regions as described earlier. However, a problem that is encountered is that mode 1 crack opening does not occur when the crack is under compression. Thus, the composite laminate has a different stiffness depending on the state of stress. This phenomenon is known as bimodularity.[18–21]

For static problems, bimodularity can be addressed by using an iterative technique. The neutral axis, the location in the z direction where the stress is zero, is first assumed, and compressive stiffness properties are applied to the layers under compression and tensile stiffness properties are applied to the layers under tension. The displacements are then determined, and a new neutral axis is calculated. The stiffness matrix is recalculated using the new value, and the problem is solved again. The iteration continues until the neutral axis converges to a final value. For the case of matrix cracking, not many iterations are required because the difference in overall laminate stiffness for varying locations of the neutral axis is relatively small, compared to the bimodularity that results in such materials as Kevlar®–rubber composites.

When solving for plate vibration, the nonlinearity associated with the bimodularity of matrix cracking means that superposition of vibration modes is not applicable. Natural frequency values can no longer be calculated using standard eigenvalue analysis because the plate stiffness is dependent on the deflection shape or, more specifically, whether the plate is in compression or tension. The natural frequencies can be solved for individually if the mode shape is known and used to calculate the correct stiffness matrix. Fortunately, the bimodularity introduced by matrix cracking is relatively small and results in only very small changes in the mode shape from the uncracked case to the case with matrix cracks. To demonstrate this, the technique of Wu et al.[21] is used to solve a transfer matrix model of a cantilever beam with matrix cracks. The natural frequency is calculated assuming different locations for the inflection points, and the local maximum or minimum represents the actual natural frequency. The results are shown for a $[0, 90_2]_{2s}$ glass-epoxy laminate with saturation cracking in all of the 90-deg layers ($\rho_k = 1.0$). This model was chosen because matrix cracking has a large effect in glass-epoxy and laminates with a large number of 90-deg plies. Figure 5 shows the results corresponding to the second mode of vibration. The symbol ◇ represents the inflection point for the uncracked laminate, and it is apparent that the inflection point has shifted only a very small distance. Also, the error introduced in the natural frequency, if the calculations were made using the uncracked mode shape, is on the order of 0.01%. This is so small because near the inflection point, the bending stresses are always small and small changes in the stiffness have little effect. The third mode, shown in Fig. 6, demonstrates similar behavior. However, in this case, there are two inflection points, which result in a surface plot. Again, the

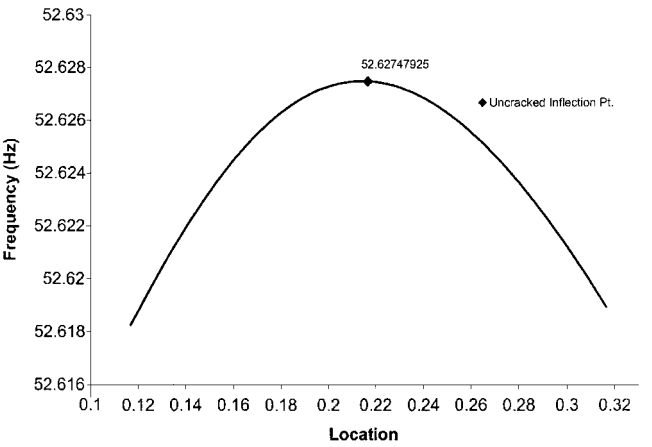

Fig. 5 Natural frequency for mode 2 inflection point location for $[0, 90_2]_{2s}$ glass-epoxy laminate.

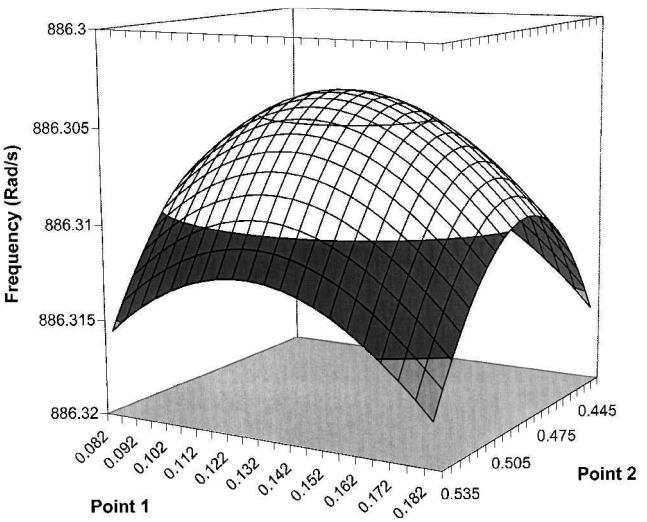

Fig. 6 Natural frequency for mode 3 inflection point location for $[0, 90_2]_{2s}$ glass-epoxy laminate.

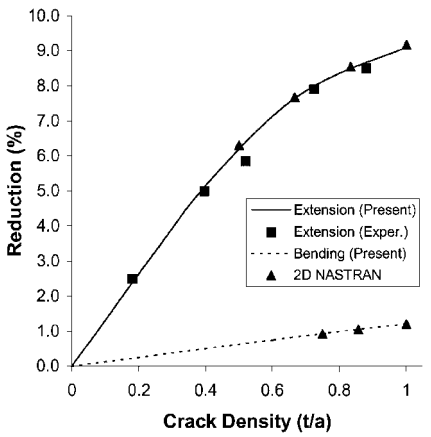

Fig. 7 Stiffness loss of graphite-epoxy $[0, 90_2]_s$ laminate.

shift in inflection point locations is small and has little effect on the calculated natural frequency.

The results from this model show that good estimates of the natural frequency can be obtained by using the uncracked mode shapes in the calculation of the stiffness matrix. The accuracy is further improved by using an iterative process during the natural frequency calculation where the uncracked mode shape is used as an initial starting point in the calculation of the stiffness matrix. The natural frequency and mode shape are determined next using eigenvalue analysis, and the new mode shape is used to recalculate the stiffness matrix. This process is continued until convergence of the inflection points and neutral axes are achieved.

During plate vibration, bimodularity can create further complexities if varying amounts of cracking exist in each of the different layers. In such a case, the structure will have different stiffness depending on whether the plate is being bent up or down. Thus, the period for each half-cycle during vibration at a natural frequency is different, and the overall natural frequency ω is determined by

$$\omega = 2\left|\left(\omega_1^{-1} + \omega_2^{-1}\right)\right. \tag{21}$$

where ω_1 and ω_2 are the natural frequencies for each half-cycle.[18] In other words, to calculate the overall natural frequency ω, the plate is analyzed first for the upward deflection case ω_1, and then again for the downward deflection case ω_2.

V. Results

The developed model is used to model sample composite plates for comparison with published experimental results. Results show that this technique accurately predicts the reduction in stiffness for a variety of materials and laminate configurations. Shown in Figs. 7 and 8 are the reductions in extensional and bending stiffness for cracked laminates of $[0, 90_2]_s$ graphite-epoxy and $[0, 90_3]_s$ glass-epoxy, respectively. The results obtained from the present model are compared with the experimental results from Refs. 17 and 22. Though the stiffnesses of the two composite materials are very different, the present model shows good correlation in both cases.

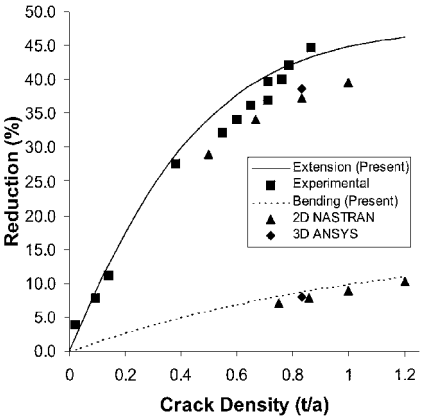

Fig. 8 Stiffness loss of glass-epoxy $[0, 90_3]_s$ laminate.

Because of a lack of sufficient experimental data on the effects of bending in the literature, ANSYS finite element models are used for validation. Finite element modeling of a cracked structure is difficult to accomplish effectively and efficiently, thus motivating the current research. Individual matrix cracks are spaced apart by a distance on the order of one or two ply thicknesses; thus, a single composite specimen will likely have hundreds of matrix cracks. The desire for accurate results motivates the modeler to use a fairly large number of elements in the vicinity of each crack and particularly near the tips. The geometry of the crack and the variety of loading possibilities motivates the use of a three-dimensional analysis. Such a model would result in a very large number of degrees of freedom. Thus for verification two slightly simplified NASTRAN and ANSYS models are used. The first is a two-dimensional plane strain NASTRAN model of the cross section of a composite laminate containing a small number of matrix cracks. The spacing of the cracks is varied slightly to reflect a realistic distribution. The plate model is then loaded and the average strains are compared to the results from an uncracked model of the same composite cross section. The second model is a three-dimensional ANSYS mesh of a single representative crack. The rational behind this model is a comparison vs the plane strain assumption. The size of this model is considerably larger in spite of modeling a single crack, and enforcement of the boundary conditions involved significant effort.

The reduction in bending stiffness is significantly smaller compared to the reduction in extensional stiffness because the matrix crack opening is much smaller during bending than it is during extension. Because of this, models that are designed for predicting extensional stiffness should not be used to determine bending stiffness. Figure 9 presents a comparison of the present model with the other available techniques.[1,2,5,17] The present model correlates well with the experimental results and asymptotically approaches the ply discount method. Unlike Hashin's method,[2] the present approach is applicable to any laminate configuration.

Figure 10 shows the reduction in stiffness for a $[0, \pm 45]_s$ glass-epoxy laminate. Again the current model has good agreement with the experimental data,[23] even in the presence of increased in-plane shear forces due to the angle plies. Figure 11 presents the reduction in the shear modulus for a $[0, 90_2]_s$ graphite-epoxy cross-ply laminate with cracking in the inner layer. Once again there is good correlation with available experimental data.[7]

Figure 12 shows the effect of matrix crack density on natural frequency for the same $[0, 90_2]_{2s}$ glass-epoxy cantilever plate already discussed. The first case is for cracking only in the upper 90-deg layer and the second case is for cracking in all 90-deg layers. The asymmetric amount of cracking in case 1 results in differing frequencies for each half-cycle (ω_1 and ω_2 in Fig. 12). This effect is most apparent for mode 1, where all of the cracks are closed

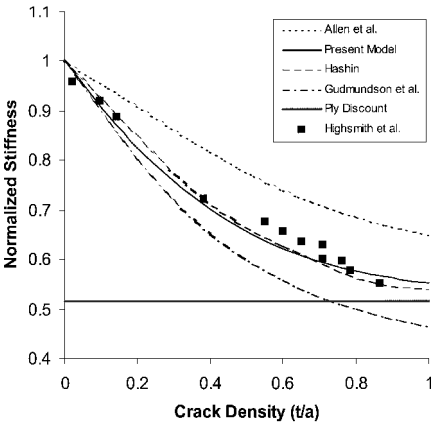

Fig. 9 Normalized extensional stiffness of glass-epoxy $[0, 90_3]_s$ laminate.

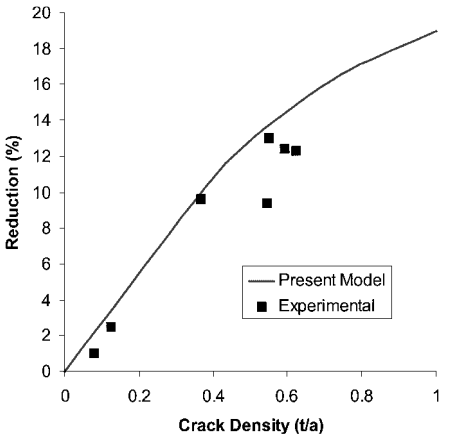

Fig. 10 Extensional stiffness loss of $[0, \pm 45]_s$ glass-epoxy laminate.

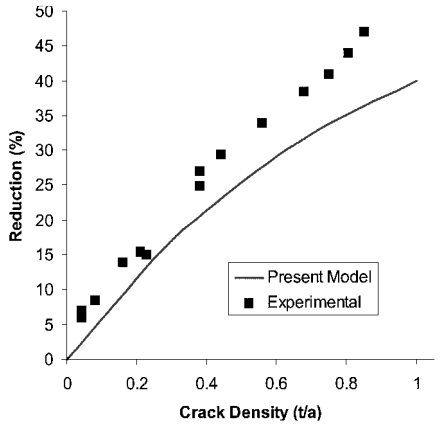

Fig. 11 Reduction in shear modulus of $[0, 90_2]_s$ graphite-epoxy laminate.

during the upward deflection ω_1. Because the cracks close, their only effect is on transverse shear, and they have little effect on natural frequency. During the downward deflection ω_2 all of the cracks open causing a significant loss in stiffness, thus reducing the natural frequency. For case 2, because the cracking is symmetric, the upward and downward deflections have the same behavior, and the half-cycles do not have different frequencies. For the higher modes, the upward and downward deflections create both areas with closed cracks and areas with open cracks, thus decreasing the difference in the two half-cycle frequencies.

Next, results are presented for cases where matrix cracks are accompanied by delamination. Figure 13 shows an example of how matrix cracking can have significant effect on structural behavior

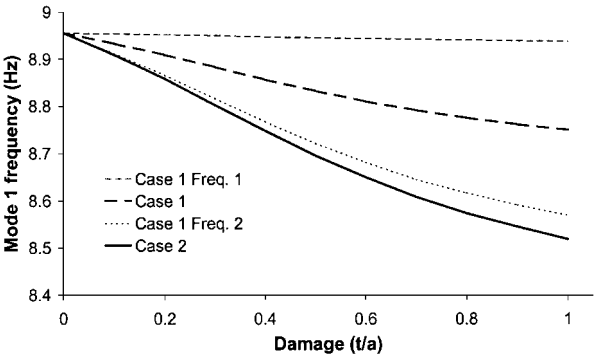

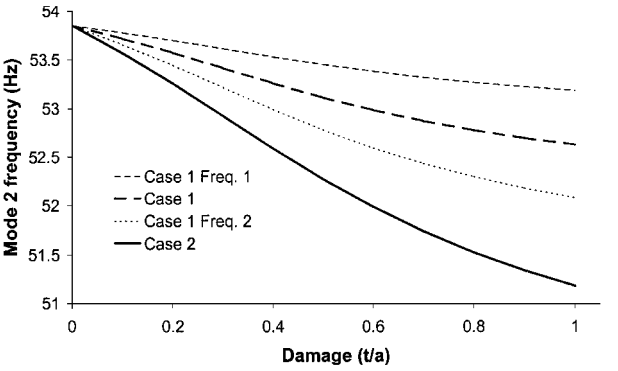

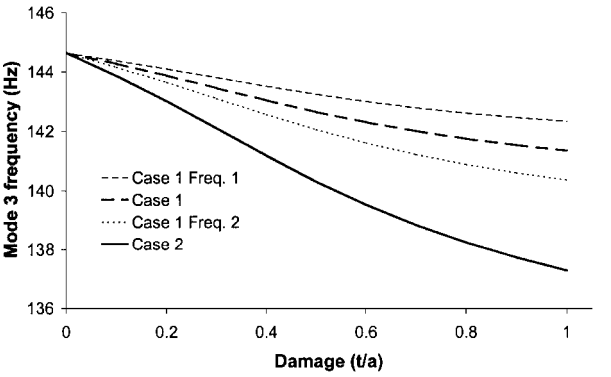

Fig. 12 Effect of matrix cracking on natural frequencies for a $[0, 90_2]_{2s}$ glass-epoxy cantilever plate.

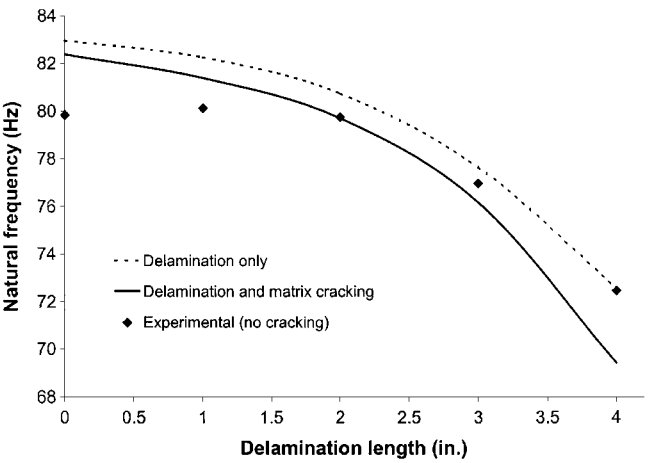

Fig. 13 Natural frequency of a delaminated graphite-epoxy $[0, 90_2]_{2s}$ cantilever plate.

that is often not considered. Shown in Fig. 13 is the effect of delamination in a $[0, 90]_{2s}$ graphite-epoxy cantilever plate, as measured by Shen and Grady.[16] The example shown is for a through the width delamination between the first 90-deg layer and the second 0-deg layer. Results are shown for the case of no matrix cracks and the case of cracking in all 90-deg layers ($\rho = 1.0$). The present theory uses a finite element mesh with 40 elements and 504 degrees of freedom. It can be seen that the effect of matrix cracking is comparable in magnitude to the effect of the delamination. Also, delamination area increases the effect of matrix cracking, as seen by a larger reduction in natural frequency at high delamination lengths. This is because the delamination creates a new surface within the laminate and cracks originally internal to the laminate are now on the surface, which dramatically increases their effect on stiffness. This example shows that matrix cracking and delamination need to be addressed simultaneously when studying the effect of damage on composite laminates.

VI. Conclusions

A unified theory has been developed to model the behavior of composite laminates with delamination and transverse matrix cracking. A higher-order displacement field was used in the sublaminates for accurate representation of the effects of transverse shear. This allowed the description of independent displacement fields above and below the delamination. A refined displacement field was obtained through the satisfaction of stress-free boundary conditions at all free surfaces, including delaminated interfaces. A finite element model was developed to describe the effect of matrix cracking using a representative crack. This was implemented into the structural model by means of reduced laminate stiffnesses. Matrix crack closure creates a bimodularity where stiffness under compression is greater than stiffness under tension. This bimodularity was addressed using an iterative process. The effect of this bimodularity on mode shapes was shown to be small, and a method was presented for determining natural frequencies in the presence of matrix cracks. Results were shown indicating that the developed model provides a consistent level of accuracy for a variety of laminate materials and configurations, with various combinations of delaminations and matrix cracks. The following important observations were made from this study:

1) The impact of all three modes of crack behavior on the overall stiffness of composite laminates with transverse matrix cracking can be modeled without the use of experimental data.

2) The nonlinearity introduced by matrix cracking is relatively small and can easily be dealt with using iterative techniques.

3) Delamination and matrix cracking cause similar reductions in the natural frequencies of composite plates.

4) Delamination can increase the effect of matrix cracks by creating new surfaces within the laminate, thus moving cracks to surface layers or closer to the surface.

Appendix: Geometric Parameters

The geometric parameters used to satisfy the continuity conditions are as follows:

$$\begin{aligned}\alpha^d = {} & [-4a^4 - 36a^3b - 60a^2b^2 - 36ab^3 - 4b^4 + 36a^2(c^u)^2 \\ & + 68ab(c^u)^2 + 36b^2(c^u)^2 + 52a^3c^d + 228a^2bc^d + 228ab^2c^d \\ & + 52b^3c^d - 72a^2c^uc^d - 136abc^uc^d - 72b^2c^uc^d - 140a(c^u)^2c^d \\ & - 140b(c^u)^2c^d - 156a^2(c^d)^2 - 388ab(c^d)^2 - 156b^2(c^d)^2 \\ & + 280ac^u(c^d)^2 + 280bc^u(c^d)^2 + 140(c^u)^2(c^d)^2 + 140a(c^d)^3 \\ & + 140b(c^d)^3 - 280c^u(c^d)^3 - 27a^2h^2 - 51abh^2 - 27b^2h^2 \\ & + 105ac^dh^2 + 105bc^dh^2 - 105(c^d)^2h^2]/\{3[9a^2 + 17ab \\ & + 9b^2 - 35ac^d - 35bc^d + 35(c^d)^2]h^2\}\end{aligned}$$

$$\begin{aligned}\beta^d = {} & (18a^2 + 34ab + 18b^2 - 35ac^u - 35bc^u - 35ac^d - 35bc^d \\ & + 70c^uc^d)(b-a)^2/\{2[9a^2 + 17ab + 9b^2 - 35ac^d - 35bc^d \\ & + 35(c^d)^2]h^2\}\end{aligned}$$

$$\begin{aligned}\delta^d = {} & [-30a^3c^u - 110a^2bc^u - 110ab^2c^u - 30b^3c^u + 72a^2(c^u)^2 \\ & + 136ab(c^u)^2 + 72b^2(c^u)^2 + 30a^3c^d + 110a^2bc^d + 110ab^2c^d \\ & + 30b^3c^d + 56a^2c^uc^d + 168abc^uc^d + 56b^2c^uc^d - 280a(c^u)^2c^d \\ & - 280b(c^u)^2c^d - 128a^2(c^d)^2 - 304ab(c^d)^2 - 128b^2(c^d)^2 \\ & + 140ac^u(c^d)^2 + 140bc^u(c^d)^2 + 280(c^u)^2(c^d)^2 + 140a(c^d)^3 \\ & + 140b(c^d)^3 - 280c^u(c^d)^3 - 18a^2h^2 - 34abh^2 - 18b^2h^2 \\ & + 70ac^dh^2 + 70bc^dh^2 - 70(c^d)^2h^2 + 18a^2(b-a)^2 \\ & + 34ab(b-a)^2 + 18b^2(b-a)^2 - 35ac^u(b-a)^2 \\ & - 35bc^u(b-a)^2 - 35ac^d(b-a)^2 - 35bc^d(b-a)^2 \\ & + 70c^uc^d(b-a)^2]/\{2[9a^2 + 17ab + 9b^2 - 35ac^d - 35bc^d \\ & + 35(c^d)^2]h^2\}\end{aligned}$$

Acknowledgment

This research was supported by the Air Force Office of Scientific Research, Grant F49620-97-1-0419; Technical Monitor, Daniel Segalman.

References

[1] Allen, D. H., and Lee, J.-W., "Matrix Cracking in Laminated Composites Under Monotonic and Cyclic Loadings," *Composites Engineering*, Vol. 1, No. 5, 1991, pp. 319–334.

[2] Hashin, Z., "Analysis of Stiffness Reduction of Cracked Cross-Ply Laminates," *Engineering Fracture Mechanics*, Vol. 25, No. 5/6, 1986, pp. 771–778.

[3] Smith, P. A., and Wood, J. R., "Poisson's Ratio as a Damage Parameter in the Static Tensile Loading of Simple Cross-Ply Laminates," *Composite Science and Technology*, Vol. 38, No. 1, 1990, pp. 85–93.

[4] Makins, R. K., and Adali, S., "Bending of Cross-Ply Delaminated Plates With Matrix Cracks," *Journal of Strain Analysis for Engineering Design*, Vol. 26, No. 4, 1991, pp. 253–257.

[5] Adolfsson, E., and Gudmundson, P., "Thermoplastic Properties in Combined Bending and Extension of Thin Composite Laminates with Transverse Matrix Cracks," *International Journal of Solids and Structures*, Vol. 34, No. 16, 1997, pp. 2035–2060.

[6] Smith, P. A., and Ogin, S. L., "On Transverse Matrix Cracking in Cross-Ply Laminates Loaded in Simple Bending," *Composites: Part A*, Vol. 30, No. 8, 1999, pp. 1003–1008.

[7] Tsai, C.-L., and Daniel, I. M., "The Behavior of Cracked Cross-Ply Composite Laminates Under Shear Loading," *International Journal of Solids and Structures*, Vol. 29, No. 24, 1992, pp. 3251–3267.

[8] Gudmundson, P., and Zang, W., "An Analytical Model for Thermoplastic Properties of Composite Laminates Containing Transverse Matrix Cracks," *International Journal of Solids and Structures*, Vol. 30, No. 23, 1993, pp. 3211–3231.

[9] Yang, H. T. Y., and He, C. C., "Three-Dimensional Finite Element Analysis of Free Edge Stresses and Delamination of Composite Laminates," *Journal of Composite Materials*, Vol. 28, No. 15, 1994, pp. 1394–1412.

[10] Kardomateas, G. A., and Schmueser, D. W., "Buckling and Postbuckling of Delaminated Composites Under Compressive Loads Including Transverse Shear Effects," *AIAA Journal*, Vol. 26, No. 3, 1988, pp. 337–343.

[11] Pavier, M. J., and Clarke, M. P., "A Specialized Composite Plate Element for Problems of Delamination Buckling and Growth," *Composite Structures*, Vol. 35, No. 1, 1996, pp. 45–53.

[12] Barbero, E. J., and Reddy, J. N., "Modeling of Delamination in Composite Laminates Using a Layer-Wise Plate Theory," *International Journal of Solids and Structures*, Vol. 28, No. 3, 1991, pp. 373–388.

[13] Chattopadhyay, A., and Gu, H., "New Higher-Order Plate Theory in Modeling Delamination Buckling of Composite Laminates," *AIAA Journal*, Vol. 32, No. 8, 1994, pp. 1709–1718.

[14] Chattopadhyay, A., and Gu, H., "Elasticity Solution for Delamination Buckling of Composite Plates," *Proceedings of the 37th AIAA/ASME/ASCE/AHS/ASC Structures, Structural Dynamics, and Materials Conference*, AIAA, Reston, VA, 1996, pp. 2543–2551.

[15] Chattopadhyay, A., and Gu, H., "An Experimental Investigation of Delamination Buckling and Postbuckling of Composite Laminates," *Composites Science and Technology*, Vol. 59, No. 6, 1999, pp. 903–910.

[16] Shen, M. H. H., and Grady, J. E., "Free Vibrations of Delaminated Beams," *AIAA Journal*, Vol. 30, No. 5, 1992, pp. 1361–1370.

[17]Highsmith, A. L., and Reifsnider, K. L., "Stiffness Reduction Mechanisms in Composite Laminates," *Damage in Composite Materials*, edited by K. L. Reifsnider, ASTM STP 775, American Society for Testing and Materials, Bal Harbour, FL, 1982, pp. 103–117.

[18]Bert, C. W., Reddy, J. N., Chao, W. C., and Reddy, V. S., "Vibration of Thick Rectangular Plates of Bimodulus Composite Material," *Journal of Applied Mechanics*, Vol. 48, No. 2, 1981, pp. 371–376.

[19]Reddy, J. N., "Transient Response of Laminated, Bimodular-Material, Composite Rectangular Plates," *Journal of Composite Materials*, Vol. 16, March 1982, pp. 139–152.

[20]Tseng, Y. P., and Bai, K. P., "Bending Analysis of Bimodular Laminates Using a Higher-Order Plate Theory With the Finite Element Technique," *Computers and Structures*, Vol. 47, No. 3, 1993, pp. 487–494.

[21]Wu, J. S., Jing, H. S., and Cheng, C. R., "Free-Vibration Analysis of Single-Layer and Two- Layer Bimodular Beams," *International Journal for Numerical Methods in Engineering*, Vol. 28, No. 4, 1989, pp. 955–965.

[22]Groves, S. E., "A Study of Damage Mechanics in Continuous Fiber Composite Laminates With Matrix Cracking and Interply Delaminations," Ph.D. Dissertation, Aerospace Engineering Dept., Texas A&M Univ., College Station, TX, May 1986.

[23]Highsmith, A. L., Stinchcomb, W. W., and Reifsnider, K. L, "Stiffness Reduction Resulting From Transverse Matrix Cracking in Fiber-Reinforced Composite Laminates," Engineering Science and Mechanics Dept., Rept. VPI-E-8133, Virginia Polytechnic Inst. and State Univ., Blacksburg, VA, Nov. 1981.

A. M. Waas
Associate Editor